

# Predicting Multiscale Strain Transfer and ECM Stress Transmission during Healing and Dynamic Loading in Tendon

Benjamin Freedman, PhD<sup>1,2,3</sup>

Ehsan Ban<sup>4</sup>

Ashley Rodriguez<sup>1</sup>

Joseph Newton<sup>1</sup>

Ryan Leiphart<sup>1</sup>

Vivek Shenoy<sup>4</sup>

Louis Soslowsky, PhD<sup>1</sup>

<sup>1</sup>McKay Orthopaedic Research Laboratory  
University of Pennsylvania

<sup>2</sup>John A. Paulson School of Engineering and  
Applied Sciences  
Harvard University

<sup>3</sup>Wyss Institute for Biologically Inspired  
Engineering  
Cambridge, MA

<sup>4</sup>Materials Science  
University of Pennsylvania

## Introduction

The extracellular matrix (ECM) is a major component of the biomechanical environment with which tendon cells (tenocytes) interact (Fig.1). Dynamic reciprocity between ECM and cell forces can affect many cell responses (e.g., inflammation, migration, proliferation, and differentiation), cell-cell communication, and tissue patterning/re-arrangement [1]. Although loading induced changes in gene and protein expression have been studied in tendon [2], appreciation for how applied strains result in nuclear shape changes that may drive these downstream responses remains limited. The ability or hindrance of cells to deform under applied strain may have important physiological consequences and may be a potential therapeutic target. Therefore, the objectives of this study were to (1) predict nuclear strain transfer in tendon from multiscale mechanical, structural, and compositional properties during healing and after perturbations of dynamic loading using multiple regression models and (2) apply a constitutive model to elucidate the role of dynamic mechanical loading and tendon healing on the ability for tenocytes to sense stress over long distances. We hypothesized that the nuclear aspect ratio (nAR) and  $\Delta$ nAR would be predicted by strain stiffening, collagen disorganization, and cellularity and that healing and high dynamic loading would decrease ECM stress transmission.

## Methods

### Study Design

Female C57BL/6 mice at 150 days of age were randomized into uninjured controls (n=75 mice) and those that received bilateral excisional injuries (n=88 mice) to their patellar tendons (IACUC approved). Injured animals were randomized into groups euthanized at 2 or 6 weeks post-injury.

### Ex vivo Assays

Tendons were harvested immediately and prepared for mechanical testing under aseptic conditions to maintain cell viability. Tendons (n=10-13/

group) were preconditioned, randomized into zero, low, or high magnitude loading protocols (corresponding to the toe or linear regions of the force-displacement curve) for 1000 cycles at 1Hz prior to dynamic mechanical analysis, and ramped at constant strain rate to 1% or 10% strain. Force and displacement data were used to compute several mechanical properties ( $|E^*|$ ,  $\tan\delta$  equilibrium stress  $\sigma_{eq}$ ). The same tendons were snap frozen at 1% or 10% strain and cryosectioned for multiphoton imaging to evaluate collagen fiber disorganization (circular standard deviation (CSD)), cellularity, F-actin, nuclear aspect ratio (nAR), and nuclear disorganization (nCSD).

### Multiple Regression

Assumptions for linear analysis were satisfied. Pearson's correlations were calculated between independent variables. Backward linear regression was performed (F to enter: 0.05, removed: 0.10) to predict nAR and  $\Delta$ nAR.

### Constitutive Modeling

A constitutive law for fibrous matrices was applied to model stress transmission in tendon using experimental inputs. Finite- element simulations of this constitutive law were used to study the effect of material properties of the isotropic ( $E_b$ ) and fibrous ( $E_f$ ) components of the matrix, the shape of cells, and the polarization of cell contractile forces on force transmission in fibrous matrices in response to dynamic loading and healing. Briefly, two distinct groups of aligned and isotropic fibers were incorporated: (1) Isotropic fibers were modeled as neo-Hookean hyperelastic and (2) energy functions describing

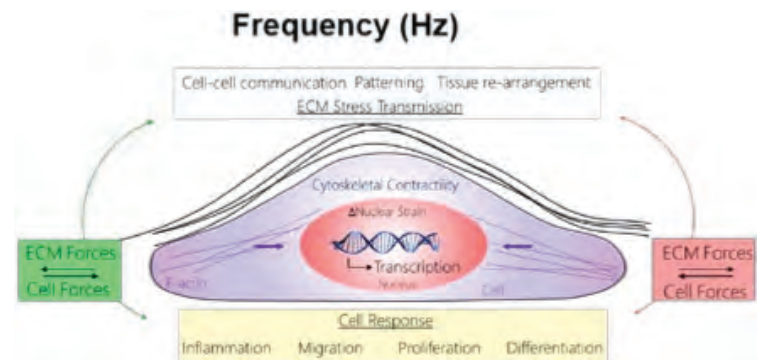


Figure 1. ECM and cell forces can have important physiological consequences.

**Table 1: Correlations to nAR**

		$\sigma_{eq}$	$ E^* $	Cellularity	F-actin	CSD	nCSD	Heal
nAR	R-Value	0.40	0.33	-0.74	-0.83	-0.85	-0.81	-0.89
	Sig. (2-tail)	<0.001	<0.001	<0.001	<0.001	<0.0001	<0.001	<0.001
	N	91	172	176	170	178	175	181

aligned fibers were chosen so that the tendon matrix increases in stiffness under tensile loading [3]. A 3D 1-element model was constructed with tendon-specific geometries in Abaqus/CAE to determine the model parameters. A 3D axis-symmetric model was used (Mesh size: 1-6 $\mu$ m) to evaluate ECM stress transmission. Cells contracted up to 5% of their volume along their principal axis. During cell contraction, the maximum principal stresses, nodal displacements, and nodal coordinates were output and analyzed in MATLAB (v2012a; Mathworks; Natick, MA).

## Results

Bivariate correlation revealed that  $\sigma_{eq}$ ,  $|E^*|$ , cellularity, F-actin staining, CSD, nCSD, and healing correlated with nAR, with correlation coefficient magnitudes ranging from  $r=0.33$  to  $r=0.85$  (Table 1). Using these parameters, backward linear regression determined that cellularity, nuclear disorganization, and healing were significant predictors of nAR ( $R^2=0.85$ ,  $p<0.001$ ). Bivariate correlation determined that  $\Delta\sigma_{eq}$ ,  $\tan\delta$ , cellularity, F-actin,  $\Delta$  nCSD, healing, and high magnitude loading were significantly correlated with  $\Delta$ nAR (indicates the capacity for nuclei to deform under applied loading). The categorical variables healing and fatigue loading were the strongest predictors of  $\Delta$ nAR ( $R^2=0.39$ ,  $p<0.001$ ). In the constitutive model, healing tendon demonstrated decreased displacement transmission profiles compared to uninjured intact tendon (Fig.2). Additionally, fatigue loaded tendon displacement profiles decayed rapidly within short distances from the cell surface.

## Discussion

This study determined that multiscale mechanical, structural, and compositional properties could predict nuclear strain transfer and investigated the effects of healing and dynamic loading on tendon cell stress transmission through the ECM. nAR was strongly correlated with several macroscale and microscale properties, highlighting its relationship to multiscale tendon properties. nAR was most correlated to nCSD and F-actin staining. Interestingly, the  $\Delta$ nAR in healing tendon was primarily correlated to matrix mechanical properties and cellular properties, whereas the  $\Delta$ nAR in dynamically loaded tendon was primarily correlated to macroscale mechanical properties and nuclear organization. Therefore, it is likely that the mechanisms of nuclear strain transfer are inherently fundamentally different between these groups. Additionally,

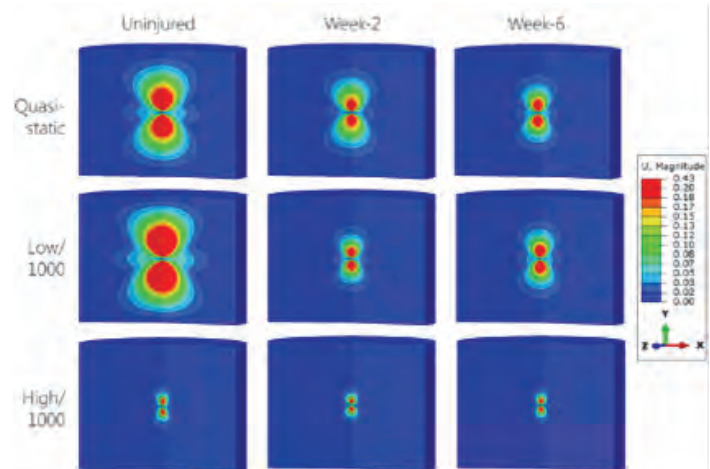


**Figure 2.** Displacement profiles comparing the effect of healing and cyclic loading ECM stress transmission]

tendon healing and fatigue loading drastically decreased simulated stress transmission compared to uninjured control tendons. These large differences are likely due to an elongated toe-region resulting from fatigue loading. Knowledge gained from these models may advance our understanding for cell-ECM and cell-cell communication within tendon throughout healing and in response to dynamic loading, and will provide further insight into the role of rehabilitation on tendon following injury.

## Significance

Combined experimental and modeling approaches showed that tendon healing and dynamic loading affect stress transmission in tendon. This work predicts the mechanical, structural, and compositional properties that contribute to the dynamic capacity of tendon nuclei to respond to loading.

## Acknowledgement

Research was supported by the NIH (P30AR050950, T32AR007132) and the NSF GRFP. We thank C Hillin and S Weiss.

## References

1. Mammoto A+ 2012. *J Cell Sci* 125:3061-73.
2. Legerlotz K+ 2013. *SJMSS* 23:31-7.
3. Wang H+ 2014. *Biophys J* 107:2592-2603.